

Analysis of Acoustic-Structure Interaction Case, Modelling and Possible Validation

*Original*

Analysis of Acoustic-Structure Interaction Case, Modelling and Possible Validation / Fabbri, Daniele; Rosso, Carlo; Bruzzone, Fabio. - 9:(2025), pp. 93-102. ( 43rd IMAC, A Conference and Exposition on Structural Dynamics 2025 Orlando (USA) 10 - 13 February 2025) [10.13052/97887-438-0154-2\_11].

*Availability:*

This version is available at: 11583/3004437 since: 2025-10-24T12:02:43Z

*Publisher:*

River Publishers

*Published*

DOI:10.13052/97887-438-0154-2\_11

*Terms of use:*

This article is made available under terms and conditions as specified in the corresponding bibliographic description in the repository

*Publisher copyright*

(Article begins on next page)

# Chapter 11

## Analysis of Acoustic-Structure Interaction Case, Modelling and Possible Validation



Daniele Fabbri, Carlo Rosso, and Fabio Bruzzone

**Abstract** This paper presents the analysis of the interaction between sound and an elastic plate in the air domain. Both numerical and experimental methods will be employed to investigate the acoustic field that results from the interaction of a thin flexible structure with an incident acoustic wave. The two domains are discretized using the Finite Element Method, and the Helmholtz equation together with the elastic equation are numerically solved. In order to study the level of coupling between the two domains different types of analysis are carried out. Initially, the structure is considered rigid and a hard wall boundary condition is used for the acoustic problem solution, the second analysis included the study of the thin plate displacement when it is stressed by the acoustic pressure. Finally, a multiphysics analysis is performed to consider the movement of the thin plate caused by an incident acoustic wave, which in turn induced new sound waves in the air. To ensure a precise simulation it is necessary to have a full bidirectional coupling between the acoustic field and the structure domain. A possible setup for the experimental validation is presented in the last section of the paper

**Keywords** Multiphysics, Acoustic, Structure, Acoustic structure interaction, Finite element analysis (FEA)

### Introduction

The willingness to study more physics in the same simulation has been a challenge in recent years. A fascinating and old example is the study of the interaction between a fluid and a structure, one of the most intriguing areas in multiphysics, yet it remains broad, complex, and not fully understood.

Fluid-Structure Interaction (FSI) has a lot of different fields of application as biomechanics [1], which focuses on developing and verifying novel algorithms for accurately predicting hemodynamics in major arteries. Finite element (FE) simulations are used to model the interaction between blood flow and the deformation of arterial walls, especially in a healthy aorta. The interaction between the vehicle's body and the fluid volume within its interior is typically studied as a noise vibration harshness (NVH) problem. In [2] an analysis of different methods used to solve the FE model has been carried out. The methods taken into account are Direct, Automated Multilevel Substructuring, AMLS, and Lanczos. They were compared using mesh refinement and the frequency of analysis investigation. Other FSI applications are: Battery Thermal Management[3], particle motion in an incompressible fluid [4]and magneto-hydrodynamics [5].

The aim of this paper is to describe a numerical model that represents acoustic structure interaction (ASI), a branch of FSI, which describes what happens when sound waves travel through a medium, such as air or water, and encounter a structure, such as a wall, diaphragm, or membrane. As explained in [6], a wave is the movement in a medium of a disturbance from one point to another and it takes place at a finite speed. A sound wave is a way of propagating energy by alternating compressed and rarefied particles, the distance between two consecutive points of the same phase is called wavelength and it is inversely proportional to its frequency. When a wave comes into contact with a structure, it causes a vibration by exerting pressure on it, the structural response can then modify the propagation of the sound waves, creating a continuous interaction between the two fields. At certain frequencies, the structure can resonate, amplifying specific sound waves, while at other frequencies, it can absorb or reflect the sound, changing its characteristics.

Some studies have been carried out in the same field. The eigenmodes and the vibro-acoustic response of the coupled system composed of a box and acoustic cavities were predicted by *Shi et al.* in [7] using an energy principle and Fourier series. They studied the dynamic behavior of the entire system and demonstrated how certain acoustic modes have a significant

---

Daniele Fabbri · Carlo Rosso · Fabio Bruzzone  
Department of Mechanical Engineering, Politecnico di Torino, TO 10129  
e-mail: [daniele.fabbri@polito.it](mailto:daniele.fabbri@polito.it); [carlo.rosso@polito.it](mailto:carlo.rosso@polito.it); [fabio.bruzzone@polito.it](mailto:fabio.bruzzone@polito.it)

impact on the structure's mode. Their work was based on [8], in which a modal coupling analysis was done to demonstrate that if two modes shapes of the uncoupled systems are well matched the difference between their resonance frequencies determines the rate of energy transfer. *Pan et Al.* demonstrate also that the resonance frequency of the coupled system differs from the corresponding acoustic mode, in particular, a structural mode with a specific resonance frequency will tend to "push away" the cavity mode with which it interacts. The same coupled system was investigated in [9] by changing the plate material, starting with elastic isotropic materials, such as steel and aluminum, and then with composite material. The effects of material, ply angle, and number of layers on the coupled vibro-acoustic characteristics of composite plate-cavity systems have been examined. The results highlighted that: the coupled fundamental frequencies were higher than the corresponding structural and acoustical frequencies for all materials, the aluminum plate-cavity system was more affected by the coupling than the steel case, and the composite plate-cavity systems are highly affected by the coupling compared to isotropic plate systems, with the increase in ply angle having a positive effect on the fundamental coupled frequencies.

Two main approaches can be used to solve a multiphysics problem: monolithic and partitioned. The first method treats fluid and solid domains as a single integrated system, which results in a system of equations that can be solved simultaneously with mesh movement. Instead, the partitioned considers the fluid and solid as separate systems linked through an interface. In [10] *Felippa and Park* explained the advantages of partitioned solution procedures, focusing also on their stability. They explained that the main cause of instability was the delayed feedback of fluid radiation damping energy from the fluid equation to the structural equation. To improve the convergence and stability of the partial solver an additional iteration loop can be used. This leads to a strongly coupled partitioned solution [11]. The partitioned approach presents two potentially significant advantages. It requires relatively few modifications to single-field analyzers, and this modularity is valuable given the current costs associated with software development, modification, and maintenance. The computational efficiency is also improved as the cost per time step of the staggered solution is approximately the same as processing the component fields separately. The staggered approach is economical advantageous when time step size restrictions are not an issue. Instead, in case of strong interaction, a monolithic approach ensures convergence and stability of the coupled solution. It consists of simultaneous procedures that solve in a single iteration loop the entire coupled system. Newton's method [12] is typically used to solve a unique system of equations, but consolidating multiple equations into a single system can lead to ill-conditioned system matrices, which can sometimes have zero entries on the diagonal. The work done by *Heil et Al.* [13] compares the two approaches in different test cases. It turns out that monolithic solvers are competitive in CPU time, even in cases with weak interaction. Instead for strongly coupled systems, the monolithic approach must be used as the partitioned tends to diverge. Nevertheless, in the case of large-scale problems, especially in three dimensions, maximizing the utility of monolithic solvers requires the availability of efficient preconditioners.

In this paper, a formulation that coupled pressure and displacement in the two physical domains and their FEM discretization is summarised in the background section. The multiphysics model and results are presented in the Analysis Section. Finally, a brief summary of the results and possible experimental setup is presented in the Conclusion.

## Background

The governing equation for the pressure in an acoustic medium in the frequency domain is the Helmholtz equation:

$$\nabla^2 P + \frac{\omega^2}{c_a^2} P = -i\rho_a \omega q \quad \text{in } \Omega_a \quad (1)$$

where:  $P$ ,  $\rho_a$  and  $c_a$  are the pressure the density of the acoustic domain, and the speed of sound, in the analysis domain  $\Omega_a$ . The angular frequency and the wavenumber are denoted by  $\omega$  and  $k$ , respectively. The Helmholtz equation can be solved using the appropriate boundary conditions, in this paper the following boundary conditions will be used:

- Sound Hard Wall Boundary condition

$$n \nabla P = 0 \quad (2)$$

- Imposed normal Impedance

$$P = \frac{iZ}{\rho_a \omega} \frac{\partial P}{\partial n} \quad (3)$$

where  $n$  is the outward unit normal to the fluid medium and  $Z$  is the acoustic impedance.

In the structural domain  $\Omega_s$  Newton's second law in the frequency domain can be described as follows:

$$\nabla \sigma = -\omega^2 \rho_s u \quad \text{in } \Omega_s \quad (4)$$

In (4)  $\sigma$  is the stress tensor,  $\rho_s$  the structural mass density and  $u$  the displacement vector while the body forces are not taken into account. Classic Neumann and Dirichlet boundary conditions are applied on the structural domain. As the paper is focused on a multiphysics model solved with a monolithic approach, for the sake of brevity the interface condition applied to  $\Omega_s$  and  $\Omega_a$  in the segregated approach will not be presented. However, to understand how it is possible to obtain a system of equations in the monolithic approach, a formulation called mixed displacement/pressure finite element will be explained. As this method is well described in [14] and [15] only some equations are reported.

The governing equations of this mixed formulation are: the relationship between stress and strain (5), the pressure and volumetric strain relationship (6) and the 2D definition of deviatoric (7) and volumetric strain (8):

$$\sigma = K\epsilon_v\delta + 2Ge \quad (5)$$

$$P = -K\epsilon_v \quad (6)$$

$$e = \epsilon - \frac{\epsilon_v}{2}\delta \quad (7)$$

$$\epsilon_v = \frac{\Delta V}{V} \quad (8)$$

With  $K$ ,  $G$  and  $\rho$  are the bulk modulus, the shear modulus, the mass density, three material properties, which should be used alternatively between the acoustic  $\Omega_a$  and the structural domain  $\Omega_s$ , instead  $\delta$  is Kronecker's operator. The basic approach of mixed displacement/pressure finite element formulations is to interpolate the displacements and pressure simultaneously. This requires that the principle of virtual work must be expressed using the independent variables  $u$  and  $P$ :

$$\int_{\Omega} \delta e^T C e d\Omega - \int_{\Omega} P \delta \epsilon_v d\Omega = \int_{\Omega} -\omega^2 \rho \delta u^T u d\Omega \quad (9)$$

$$\int_{\Omega} (p/K + \epsilon_v \delta P) d\Omega = 0 \quad (10)$$

Where the virtual displacement, the virtual deviatoric strain, the virtual strain are denoted by  $\delta u$ ,  $\delta e$ ,  $\delta \epsilon$  respectively,  $C$  is the stress-strain matrix for the deviatoric stress and strain component which must satisfy the following equation:

$$(\sigma + P\delta) = C(\epsilon - \frac{1}{2}\epsilon_v\delta) \quad (11)$$

The discretization with finite element of both acoustic domain [16], [17], [18] and structural domain [19] is well known and widely reported, so it is only explained how to apply FEM to this mixed displacement/pressure formulation. The starting point is writing displacement  $u$  using the standard shape functions matrix  $N_d$  and Pressure  $P$  using matrix  $N_p$ :

$$\hat{u} = \sum_{i=1}^{n_d} \mathbf{N}_d u_i \quad \hat{P} = \sum_{j=1}^{n_p} \mathbf{N}_p P_j \quad i = 1 \dots n_d \quad j = 1 \dots n_p \quad (12)$$

Where  $n_p$  and  $n_d$  are the number of prescribed shape functions for pressure and displacement. It is also possible to interpolate the deviatoric strain  $e$  and the volumetric strain  $\epsilon_v$  using matrices  $B_d$  and  $B_v$  as reported below:

$$e = \mathbf{B}_d \{u_i\} \quad \epsilon_v = \mathbf{B}_v \{u_i\} \quad i = 1 \dots n_d \quad (13)$$

The standard discretization of Equations 9 and 10 yields to the following linear system to be solved:

$$\begin{bmatrix} \mathbf{K}_{uu} - \omega^2 \mathbf{M}_{uu} & \mathbf{K}_{up} \\ \mathbf{K}_{up}^T & \mathbf{K}_{pp} \end{bmatrix} \begin{Bmatrix} U \\ P \end{Bmatrix} = \begin{Bmatrix} F_a \\ P_a \end{Bmatrix} \quad (14)$$

where the structural displacement and pressure vectors are denoted by  $U$  and  $P$ , respectively. The stiffness matrices for displacement and pressure, the mass matrix, and the external force vectors are denoted by  $\mathbf{K}_{uu}$ ,  $\mathbf{K}_{pp}$ ,  $\mathbf{M}_{uu}$ ,  $F_a$ ,  $P_a$  respectively, instead the coupling matrix  $\mathbf{K}_{up}$  is defined as [15]

$$\mathbf{K}_{up} = \mathbf{K}_{pu}^T = - \int_V \mathbf{B}_v^T \mathbf{N}_p dV \quad (15)$$

Solving the linear system of equations using a specific solver like MUMPS [20] or PARDISO [21] it is possible to find the unknown vectors  $U$ ,  $P$  for each frequency. In the following section the design of a multiphysics model representing acoustic structure interaction will be presented, based on the theoretical bases established.

## Analysis

The 2D axisymmetric multiphysics model presented in this section simulates the behavior of an aluminum plate, modeled as a shell, when it is excited by an incident acoustic wave generated by a loudspeaker in the air domain. The acoustic source is located at one end of a steel tube, which has a length such that the waves incident on the plate are plane, as specified by EN ISO 10534 [22]. At the other end of the pipe, a sound-absorbing material (Melamine Foam) is placed to absorb waves that might reflect at the end of the tube, thus minimizing the reflection coefficient. Eight evenly spaced flanges are welded onto the tube to secure it to mechanical supports. These flanges also need to prevent any mechanical modes of the tube within the frequency range of the plate's first natural frequency.

The purpose of this numerical model is to determine the amount of acoustic pressure transmitted when a structure is excited by an acoustic source, focusing on the range near its first natural frequency and the behavior of the transmitted pressure behind the structure. To ensure that the structure is excited by a planar wave, the pipe is designed according to the same standards used for impedance tubes, creating a controlled and consistent environment. Three different numerical models were created to determine if studying both fluid-structure interaction and acoustic behavior together is necessary. The first model, called "*1\_A.S.I.*", takes into account the interaction between the structure and the acoustic field, in a fully coupled model. The second model simplifies the system by assuming the plate as rigid, isolating the acoustic response without structural dynamics and understanding the acoustic modes of the tube, it is called "*2\_Plate\_rigid*". In "*3\_Plate\_displacement*", third and last model the acoustic source has been turned off and a prescribed displacement to the plate has been assigned, the prescribed movement of the plate derived from the acoustic-structure interaction results of the first case. This step It aids in comparing how each approach influences the transmitted pressure and evaluating the need for coupling both physics in future analyses. In Figure 1 the geometric 2D axisymmetric model built on Comsol Multiphysics is shown, the geometric dimension of the components are presented in table 1.

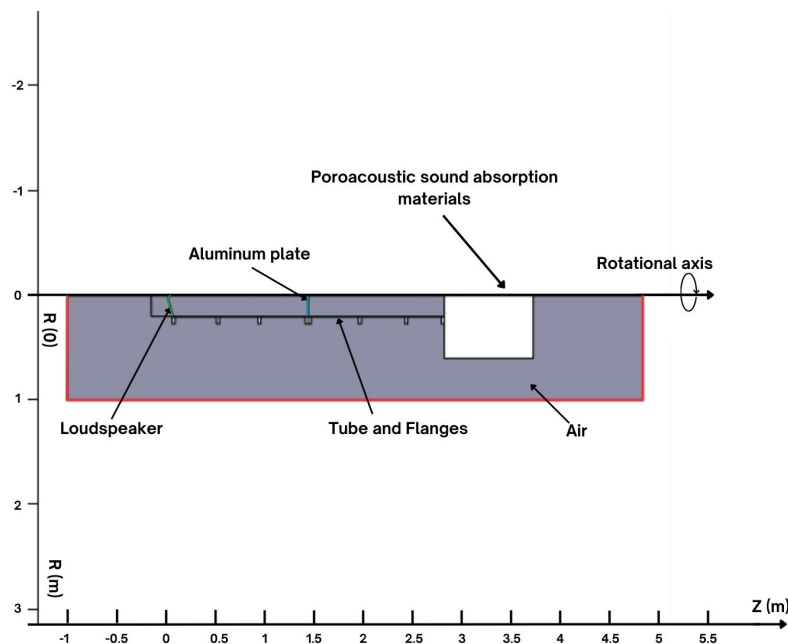


**Fig. 1** Geometric 2D axisymmetric model

The boundaries of the air domain indicated in red in Figure 1 have been assigned a perfectly matched layer boundary condition to simulate an infinite domain in which the sound waves do not reflect. A high thickness layer of melamine foam is located at one end of the pipe to limit the reflection of the wave. To accurately simulate the behavior of the poroacoustic material, a dedicated domain has been created, using the poroacoustics domain features of the Pressure Acoustics interface. The Johnson-Champoux-Allard model with a rigid frame has been selected for this purpose. This model represents an equivalent fluid model for a rigid frame porous material [23]. The melamine foam material parameters are indicated as follow: The acoustic source, a loudspeaker, is modelled as lumped system, geometrically is represented as boundary indicated in green in figure 1. This model represents a moving-coil loudspeaker, where a lumped parameter analogy is used to describe the behavior of both the electrical and mechanical components of the speaker. The coupling with the pressure acoustic

**Table 1** Geometric dimension of the model

Symbol	Value	Description
$R_1$	198.2 [mm]	Inner Tube radius
$R_2$	203.2 [mm]	Outer tube radius and inner flange radius
$R_3$	270 [mm]	Outer flange radius and plate radius
$R_4$	600 [mm]	Melamine Foam for insulating Box radius
$R_5$	190 [mm]	Loudspeaker membrane radius
$T_1$	2 [mm]	Thickness of the aluminum plate
$Z_1$	850 [mm]	Length of Melamine Foam for insulating Box
$Z_2$	2600 [mm]	Length of the tube
$Z_2$	1300 [mm]	Position of the aluminum plate

**Table 2** Melamine foam material parameters

Symbol	Value	Description
$\epsilon_p$	0.995	Porosity
$R_f$	10500 [Pa * s/m <sup>2</sup> ]	Flow resistivity
$s$	0.49 [mm]	Viscous characteristic length parameter
$L_{th}$	470 [ $\mu$ m]	Thermal characteristic length
$L_v$	240 [ $\mu$ m]	Viscous characteristic length
$\tau$	1.0059	Tortuosity factor

environment is achieved using the built-in Interior Lumped Speaker Boundary feature. The loudspeaker is modeled with an open back volume. These electric circuit models have been employed successfully for many years. The parameters that characterize a loudspeaker's low-frequency performance are commonly referred to as the Thiele-Small or small-signal parameters [24]. All parameters are constants, as they are given within the model's low-frequency limit, in table 3 the parameters associated to a commercial loudspeaker are listed.

**Table 3** Small signal parameters

Symbol	Value	Description
$M_{MD}$	56.1 [g]	Moving mass (voice coil and diaphragm)
$C_{MS}$	180e - 6 [m/N]	Suspension compliance
$R_{MS}$	2.16 [N * s/m]	Suspension mechanical losses
$BL$	22.4 [T * m]	Force factor
$R_E$	5.9 [ $\Omega$ ]	Voice coil resistance
$L_E$	0.48 [mH]	Voice coil inductance
$a$	19 [cm]	Equivalent piston radius of driver

The interaction between the two domains occurs in the part of the plate corresponding to the pipe's internal cross-section, indicated in blue in Figure 1. The aluminum plate, modeled as a shell with a thickness of 2 mm, is constrained along the entire edge, being positioned between two series of flanges which are connected by a threaded connection.

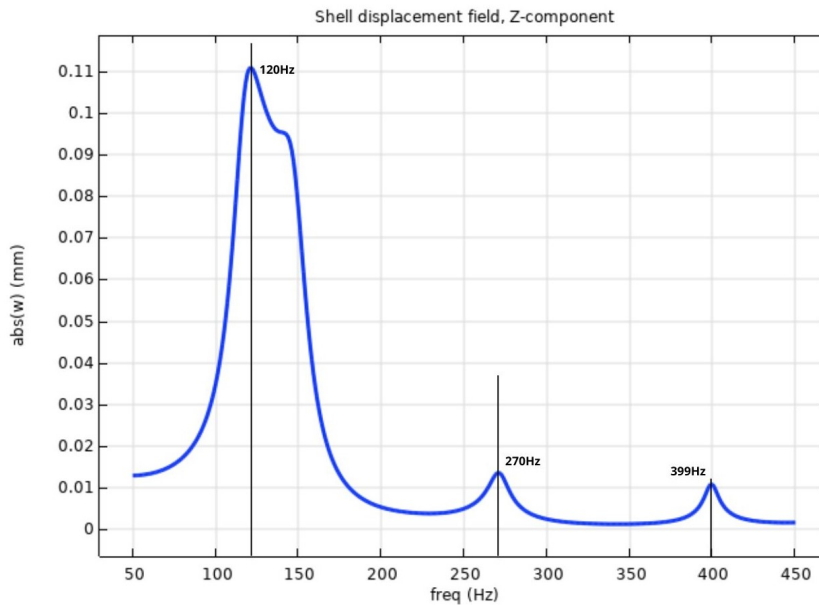
As described in [22], for an impedance tube, an upper limit, denoted as  $f_u$ , is calculated to avoid the occurrence of non-plane wave mode propagation, considering the dimensions of the pipe represents in the model, this value is 428.8 Hz. To ensure that the plate has its first natural frequency within this range, modal analysis has been conducted, the first natural frequency is at 127.93 Hz .

All the analyses were studied in the 50 – 450 Hz frequency range to be inside the plane wave region, the geometry was meshed with a 2D Finite element whose max size was 5 times smaller than the max wavelength  $\lambda$  to provide enough resolution to represent the sound field accurately. The results will be presented regarding plate displacement and acoustic pressure measured in these points inside the tube:

- ( $R = 0$  m,  $Z = 0$  m), ( $R = R_1$ ,  $Z = 0$  m) to measure the acoustic pressure at the speaker output
- ( $R = 0$  m,  $Z = 1.2$  m), ( $R = R_1$ ,  $Z = 1.2$  m) to measure the acoustic pressure before the plate in a region where the non-planar waves generated by the speaker are dissipated.

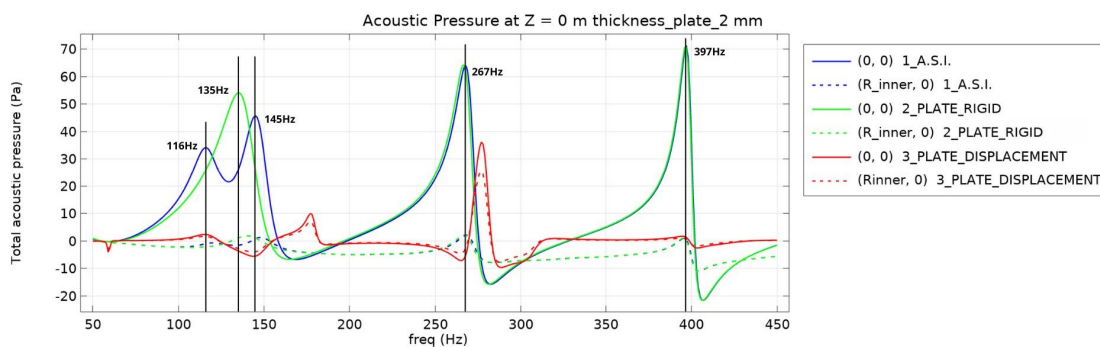
- $(R = 0 \text{ m}, Z = 2.6 \text{ m}), (R = R_1, Z = 2.6 \text{ m})$  to measure the acoustic pressure before the end of the pipe
- The Z-component displacement of the plate is measured at the center of the plate  $(R = 0 \text{ m}, Z = 1.3 \text{ m})$

Figure 2 shows the plate displacement in the 1\_A.S.I. analysis, the structural response is at  $120 \text{ Hz}$  which differs from the plate resonant frequency by more than  $7 \text{ Hz}$ , this behavior seems similar to the one described in [9] where the natural frequencies of the structure in a coupled system with a fluid cavity changes.



**Fig. 2** Plate displacement in 1\_A.S.I.

In addition to the response at the first natural frequency, there are two distinct spikes that can be explained using the acoustic pressure graphs. In figure 3 is presented the acoustic pressure measured at the speaker output  $Z = 0 \text{ m}$  at the center of the tube and the inner radius.



**Fig. 3** Acoustic pressure inside the tube at  $Z = 0 \text{ m}$ , thickness of the shell  $2 \text{ mm}$

The continuous lines represent the points at  $R = 0$  and the dotted at  $R = R_1$ , as mentioned before the waves generated by the speaker are not immediately planar, for this reason the curves do not match. Moreover, in the figure 3, it is possible to notice a difference between the first two analyses, for the first case, in which the acoustic structure interaction has been studied, two spikes of pressure in the range  $[115 - 150 \text{ Hz}]$  are present, the same trend is not replicated in the second analysis shown in green. The first peak of pressure at  $116 \text{ Hz}$  highlights the interaction between the two physics given by the movement of the plate near its coupled natural frequency which affects the acoustic field. In the rigid plate case, three

peaks of pressure occur at frequencies:  $135\text{ Hz}$ ,  $267\text{ Hz}$ , and  $397\text{ Hz}$ , to which are associated wavelengths of  $2.6\text{ m}$ ,  $1.3\text{ m}$ ,  $0.87\text{ m}$ . These peaks are related to the loudspeaker, which excites the air inside the impedance tube, at certain frequencies which coincide with the tube resonant frequencies. These resonant frequencies are determined by the tube length,  $1.3\text{ m}$ , and correspond to wavelengths that fit integer multiples of half-wavelengths within the tube. The resulting standing waves occur due to the constructive and destructive interference of the incident and reflected waves within the tube. Peaks in acoustic pressure indicate locations of antinodes, where constructive interference occurs, while nodes represent points where pressure remains zero due to destructive interference. The red lines are associated with the case in which the loudspeaker is turned off and the displacement is imposed as a boundary condition to the structure, in this case, no distinct trend can be observed comparable to the other two cases.

Figure 4 reports the acoustic pressure at  $Z = 1.2\text{ m}$ , since the case "*3\_Plate\_displacement*" did not show any significant trend, in this graph, for the sake of clarity, only the first two analyses are displayed. This figure highlights areas of low

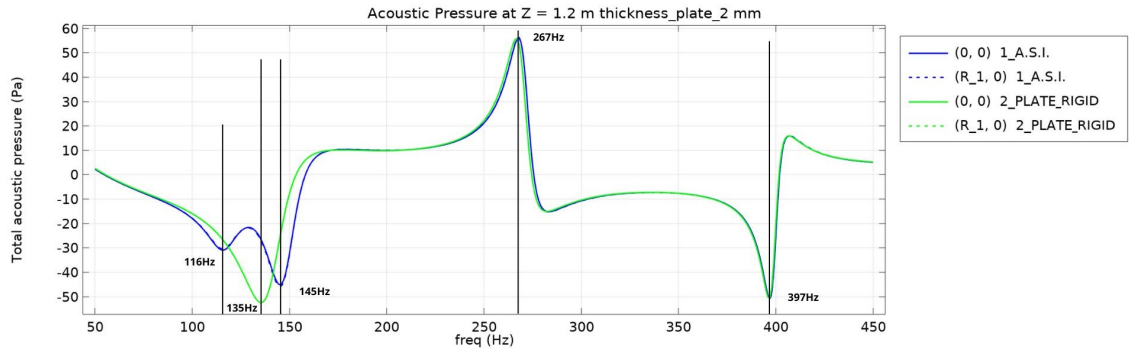


**Fig. 4** Acoustic pressure inside the tube at  $Z = 1.2\text{ m}$ , thickness of the shell  $2\text{ mm}$

pressure near the first and third acoustic resonant frequencies of the tube, also, in this case, the influence the interaction between the structure and the acoustic field is quite clear, with a similar trend to  $Z = 0\text{ m}$ , however, the curves corresponding to different radii are now superimposed because the waves have become planar.

In figure 5 is presented the case at  $Z = 2.6\text{ m}$ , all three analyses are displayed:

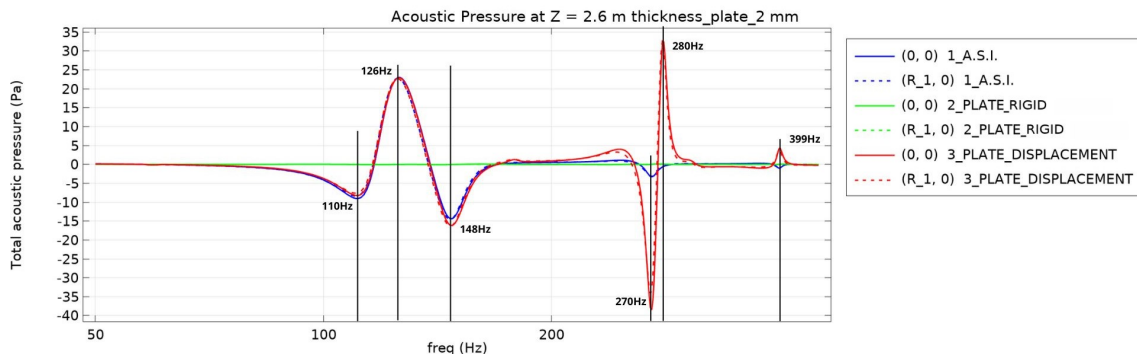


**Fig. 5** Acoustic pressure inside the tube at  $Z = 2.6\text{ m}$ , thickness of the shell  $2\text{ mm}$

It is possible to notice that in the frequency range associated with the first mode of the plate, the acoustic pressure transmitted over the tube reaches a value bigger than  $20\text{ Pa}$ , given by the coupled presence of the plate and tube resonant frequency, this is confirmed by the behavior at the other tube resonant frequencies, here high-pressure peaks do not occur. The *2\_Plate\_rigid* case shows an acoustic pressure value equal to  $0\text{ Pa}$  at all frequencies. The plate-imposed displacement case, despite a slight difference of around  $2\text{ Pa}$ , reconstructs the pressure curve in the plate resonance frequency range. However, at the tube acoustic resonant frequencies, the model produces very high values of pressure, which indicates how this analysis should be revised in more detail.

To replicate this experiment, a possible setup has been created. The dimensions are the same as those used in the multiphysics model. In the geometric model, mechanical carriers are present, even though numerically they are considered as

boundary constraints. The speaker is inside the aluminum box, but as a preliminary simulation showed some numerical errors, it will be decided in the future whether to use it with open air behind or use melamine foam inside the box to ensure proper sound insulation. The CAD model is presented in figure 6, however, there are no microphones for recording pressure, similar to those used in impedance tests, and the optical sensor for measuring plate displacement.

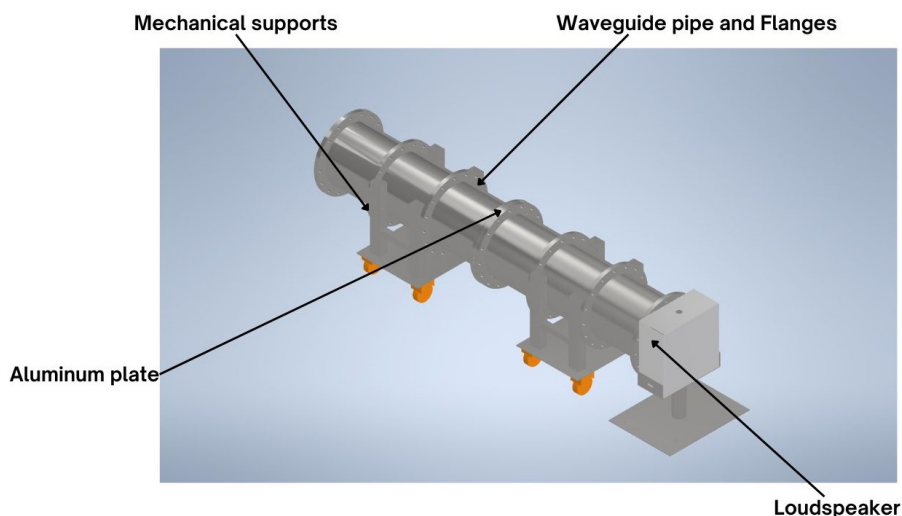


**Fig. 6** Possible experimental set-up

## Conclusion

The results of this study demonstrate the significant impact of interactions between different physical domains. The acoustic-structure interaction case shows that when a structure is excited by an acoustic source at its resonance frequency, a substantial amount of pressure is transmitted downstream of the plate, especially when the mechanical resonance frequency of the structure and the acoustic resonance frequency of the pipe are similar. The three analyses presented examined the possibility of avoiding the need for modelling multiphysics coupling. It was discovered that deviating from a multiphysics approach produced noticeable differences, however further investigations are required to fully evaluate this possibility. Furthermore, to strengthen the validity of the numerical model presented in this study, future experimental tests using the setup outlined in the last section are necessary. The purpose of these tests is to compare numerical predictions with real measurements, which will lead to a more robust framework for understanding acoustic-structure interactions and improving the model accuracy.

**Acknowledgments** This publication is part of the project PNRR-NGEU which has received funding from the MUR – DM 117/2023.

## References

1. Crosetto, Reymon, Deparis, Kontaxakis, Stergiopoulos, and Quarteroni. “Fluid–structure interaction simulation of aortic blood flow”. *Computers & Fluids*, 43(1):46–57 (2011)
2. Kropp and Heiserer. “Efficient broadband vibro-acoustic analysis of passenger car bodies using an fe-based component mode synthesis approach”. *Journal of Computational Acoustics*, 11(2):139–157 (2003)
3. Liao, Y., Xu, H., Huang, S.X., Taishuo, and Hu, Z. “Modeling of fluid-structure interaction to enhance battery thermal management in electric vehicles”. pages 14–29 (2023)
4. Koshizuka, S. and Oka, Y. “Moving-particle semi-implicit method for fragmentation of incompressible fluid”. *Nuclear Science and Engineering*, 123(3):421–434 (1996)
5. MÜCK, B., GÜNTHER, C., MÜLLER, U., and BÜHLER, L. “Three-dimensional mhd flows in rectangular ducts with internal obstacles”. *Journal of Fluid Mechanics*, 418:265–295 (2000)
6. Blackstock, D.T. *Fundamentals of physical acoustics / David T. Blackstock*. Wiley (2000)

7. Shi, S., Wang, J., Liu, K., Jin, G., and Xiao, B. "Vibro-acoustic modelling of the box structural–acoustic coupling system". *Results in Physics*, 31:104915 (2021)
8. Pan, J. and Bies, D.A. "The effect of fluid–structural coupling on sound waves in an enclosure—Theoretical part". *The Journal of the Acoustical Society of America*, 87(2):691–707 (1990)
9. Sarıgül, A.S. and Karagözlü, E. "Vibro-acoustic coupling in composite plate-cavity systems". *Journal of Vibration and Control*, 24(11):2274–2283 (2018)
10. Felippa, C. and Park, K. "Staggered transient analysis procedures for coupled mechanical systems: Formulation," *Computer Methods in Applied Mechanics and Engineering*, 24:61–111 (1980)
11. Tallec, P.L., Gerbeau, J.F., Hauret, P., and Vidrascu, M. "Fluid structure interaction problems in large deformation,". *Comptes Rendus Mécanique*, 33:910–922 (2005)
12. Galantai, A. "The theory of newton's method". *Journal of Computational and Applied Mathematics*, 124:25–44 (2000)
13. Heil, M., Hazel, A., and Boyle, J. "Solvers for large-displacement fluid–structure interaction problems: segregated versus monolithic approaches". *Computational Mechanics*, 43:91–101 (2008)
14. Yoon, G., Jensen, J., and Sigmund, O. "Topology optimization of acoustic–structure interaction problems using a mixed finite element formulation". *International Journal for Numerical Methods in Engineering*, 70:1049 – 1075 (2007)
15. Bathe, K. *Finite Element Procedures*. Prentice Hall (2006)
16. Desmet, W. and Vandepitte, D. "Finite element method in acoustics" (1999)
17. Ihlenburg, F. and Babuška, I. "Finite element solution of the helmholtz equation with high wave number part i: The h-version of the fem". *Computers & Mathematics with Applications*, 30(9):9–37 (1995)
18. Prinn, A.G. "A review of finite element methods for room acoustics". *Acoustics*, 5(2):367–395 (2023)
19. Macneal, R.H. *Finite Elements: Their Design and Performance*. DEKKER, 270, Madison Avenue, New York (1994)
20. Amestoy, P., Duff, I., and L'Excellent, J.Y. "Multifrontal parallel distributed symmetric and unsymmetric solvers". *Computer Methods in Applied Mechanics and Engineering*, 184:501–520 (2000)
21. Schenk, O. and Gärtner, K. *PARDISO*. Springer US, Boston, MA (2011)
22. International Organization for Standardization. "Iso 10534-2:2023 - acoustics — determination of acoustic properties in impedance tubes— part 2: Two-microphone technique for normal sound absorption coefficient and normal surface impedance" (2023)
23. Cao, L., Fu, Q., Si, Y., Ding, B., and Yu, J. "Porous materials for sound absorption". *Composites Communications*, 10:25–35 (2018)
24. Falaize, A. and Hélie, T. "Passive modelling of the electrodynamic loudspeaker: from the thiele–small model to nonlinear port-hamiltonian systems". *Acta Acustica*, 4:1 (2020)

